Contact Photothermal Techniques for Thermal Characterization of Liquids

D. Dadarlat*

Department of Molecular and Biomolecular Physics, National R&D Institute for Isotopic and Molecular Technologies, Donat Str. 67-103, Cluj-Napoca 5, 400293, Romania

Abstract: Two contact photothermal (PT) techniques, the well-known photopyroelectric (PPE) calorimetry, and a recently introduced photothermoelectric (PTE) one, are proposed for thermal inspection of some liquid samples. The paper contains a summary of the recent results and a comparison of the investigations performed with the previously mentioned techniques for the measurement of the dynamic thermal parameters (thermal diffusivity and effusivity) of some liquids of interest: magnetic nanofluids with transformer oil as carrier liquid and various concentrations of magnetite (Fe_3O_4) nanoparticles. For both techniques, the same detection configurations have been used: (i) the front detection configuration, together with the thermal-wave resonator cavity (TWRC) method as scanning procedure, was used to measure the value of thermal effusivity; (ii) the back configuration, together with the same TWRC technique, leads to the direct measurement of thermal diffusivity. The main theoretical aspects of the particular detection cases for both techniques are described and the performances (advantages and limitations) of the methods are analyzed. Concerning the nanofluid under investigation, small increases of thermal diffusivity (9.33 m^2s^{-1} – 10.33 m^2s^{-1}) and effusivity (450 $Ws^{1/2}$ $m^{-2}K^{-1}$ – 530 $Ws^{1/2}$ $m^{-2}K^{-1}$) with increasing nanoparticles' concentration (0.156 mg(Fe_3O_4)/ml fluid - 0.623 mg(Fe_3O_4)/ml fluid) are observed.

Keywords: Photothermal phenomena, photopyroelectric calorimetry, photothermoelectric calorimetry, liquids, thermal parameters.

1. INTRODUCTION

During the last decades, contact and non-contact photothermal (PT) techniques have been largely used for optical and thermal characterization of various condensed matter materials [1]. Among the PT contact methods, the photopyroelectric technique (PPE) is probably the most used for calorimetric purposes. In the PPE calorimetry, a sample is irradiated with an optical beam and, the heat, generated in the sample due to the absorption of radiation, is measured with a pyroelectric sensor which is in good thermal contact with the sample [2, 3]. Various detection configurations, (back and front) sources of information (amplitude and phase of the signal) and scanning parameters (chopping frequency of radiation and/or thickness of one liquid layer of the detection cell) were used, depending on the purpose of the investigation [4, 5].

Recently, it has been shown that similar results can also be obtained with thermoelectric (TE) generators too. In this case, the physical mechanism relies on the Seebeck effect. The efficiency of the device depends on material characteristics such as the Seebeck coefficient (S_0), thermal (k) and electrical (σ) conductivities. The figure of merit $zT = S_0^2\sigma T/k$ is used to compare the TE devices' performances. Kuriakose *et al*. [6] proposed this new contact photothermal technique, based on the so called photothermoelectric (PTE) effect with the main purpose of thermal characterization of TE generators. The detection configuration was similar to the front detection configuration for the PPE technique, but the pyroelectric sensor was replaced by a TE generator. The detection cell consisted of two layers and the scanning parameter was the chopping frequency of laser irradiation. This novel method allows the determination of thermal parameters such as effusivity and diffusivity of the material used as sensor. Recently, Dadarlat *et al*. [7] extended the application of thermoelectrics, by using them as radiation sensors in order to directly measure the dynamic thermal parameters of some solids.

In this paper we propose to use alternatively the PPE technique (based on a $LiTaO_3$ pyroelectric sensor) and the PTE method (based on TiS_3 as TE material) for thermal characterization of some liquid samples. The detection configurations are: (i) the "front" one (FPPE/FPTE- sensor directly irradiated and sample in back position) coupled with TWRC method (scan of the liquid's thickness) [8], for thermal effusivity measurements and (ii) the "back" one (BPPE/BPTE - sample directly irradiated and sensor in back position), together with the same scanning procedure (TWRC), for thermal diffusivity investigations [9]. The liquid sample was a magnetic nanofluid with transformer oil as carrier liquid, oleic acid as surfactant and Fe_3O_4

*Address correspondence to this author at the Department of Molecular and Biomolecular Physics, National R&D Institute for Isotopic and Molecular Technologies, Donat Str. 67-103, Cluj-Napoca 5, 400293, Romania;
Tel:+40-264-584037; Fax:+40-264-42042; E-mail:ddadarlat@gmail.com

E-ISSN: 2409-5826/14

nanoparticles. The measurements of the two dynamic thermal parameters were performed in some nano-particles' concentration range.

2. THEORETICAL ASPECTS

The schematic of the detection cells in the front/back detection configurations are presented in Figure **1**.

The theory of the two detection configurations for the two methods was largely described elsewhere [7, 10-12]. We will give here only some details and the final results.

For weak temperature variations, the voltage signal generated by the pyroelectric and thermoelectric material, respectively is given by:

-front configuration

$$V^{PPE} = \int_{-l1}^{0} T(x)\,dx \tag{1}$$

$$V^{PTE} = S_0 \int_{T=T(-l1)}^{T=T(0)} dT = S_0[T_1(x=0) - T_1(x=-l_1)] \tag{2}$$

-back configuration

$$V^{PPE} = \int_{-l1-l2}^{-l1} T(x)\,dx \tag{3}$$

$$V^{PTE} = S_0 \int_{T=T(-l1-l2)}^{T=T(-l1)} dT = S_0[T_2(x=-l_1) - T_2(x=-l_1-l_2)] \tag{4}$$

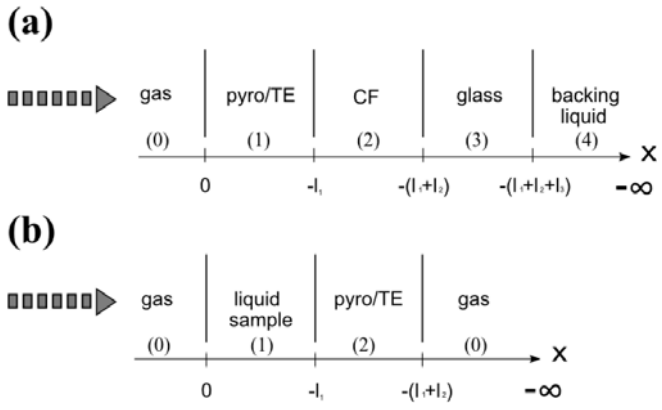

Figure 1: Schematic of the front (**a**) and back (**b**) detection cells. Gas = air; TE = thermoelectric generator; CF = coupling fluid; separator = glass.

In the following, we suppose that the detection cell is irradiated with a modulated laser beam of angular frequency ω=2πf and a fraction from its intensity is absorbed by the first irradiated layer of the cell and transformed into heat. Solving a well-known system of thermal diffusion equations [2, 3] one can calculate the temperature variation across the pyroelectric/TE sensors.

In the front configuration, if we suppose that the sensor is opaque (the optical radiation is absorbed on the first electrical contact), in the thermally thick limit for the backing liquid (the geometrical thickness is much larger than the thermal diffusion length in material), the temperature across the sensor is given by [11]:

$$T_1(x) = \frac{H_0}{2k_1\sigma_1} \frac{\left[e^{-\sigma_1 x} + \rho_{21} e^{-\sigma_1(2l_1 - x)}\right]}{1 - \rho_{21} e^{-2\sigma_1 l_1}} \tag{5}$$

Where H_0 is the incident flux and

$$\rho_{21} = \frac{(1-b_{21}) + \rho_{32}(1+b_{21}) e^{-2\sigma_2 l_2}}{(1+b_{21}) + \rho_{32}(1-b_{21}) e^{-2\sigma_2 l_2}} \tag{6a}$$

$$\rho_{32} = \frac{(1-b_{32}) + \rho_{43}(1+b_{32}) e^{-2\sigma_3 l_3}}{(1+b_{32}) + \rho_{43}(1-b_{32}) e^{-2\sigma_3 l_3}} \tag{6b}$$

$$\rho_{43} = \frac{1-b_{43}}{1+b_{43}} \tag{6c}$$

$$b_{ij} = \frac{e_i}{e_j};\ \sigma = (1+\sqrt{-1})\left(\frac{\omega}{2\alpha}\right)^{1/2} \tag{6d}$$

Inserting Eq. (5) in Eqs. (1) and (2) we obtain for the normalized FPPE and FPTE signals:

$$V_n^{FPPE} = \frac{1 - R_{21} e^{-2\sigma_1 l_1}}{1 - \rho_{21} e^{-2\sigma_1 l_1}} * \frac{\left(e^{-\sigma_1 l_1} - 1\right) - \rho_{21}\left(e^{-\sigma_1 l_1} - e^{-2\sigma_1 l_1}\right)}{\left(e^{-\sigma_1 l_1} - 1\right) - R_{21}\left(e^{-\sigma_1 l_1} - e^{-2\sigma_1 l_1}\right)} \tag{7}$$

$$V_n^{FPTE} = \frac{1 - R_{21} e^{-2\sigma_1 l_1}}{1 - \rho_{21} e^{-2\sigma_1 l_1}} * \frac{\left(e^{-\sigma_1 l_1} - 1\right) + \rho_{21}\left(e^{-\sigma_1 l_1} - e^{-2\sigma_1 l_1}\right)}{\left(e^{-\sigma_1 l_1} - 1\right) + R_{21}\left(e^{-\sigma_1 l_1} - e^{-2\sigma_1 l_1}\right)} \tag{8}$$

where

$$R_{21} = \frac{1-b_{21}}{1+b_{21}} \tag{9}$$

In Eqs. (6)- (8) e represents the thermal effusivity, α is the thermal diffusivity and R_{ij} represents the reflection coefficient of the thermal wave at the (i,j) interface. The normalization of the signal in Eqs. (7) and (8) was performed with thermally very thick coupling fluid.

Eqs. (7) – (8) indicate that the electrical signal obtained from a pyroelectric or TE sensor, inserted in a sandwiched cell as presented in Figure **1**, and periodically illuminated with an optical radiation, is a complex voltage and depends on the thermal diffusivity and effusivity of the first three layers of the detection cell (sensor, coupling fluid and separator) and on the thermal effusivity of the material situated in the backing position (layer 4). In principle, experimentally, we can perform a scanning procedure, using as scanning parameter either the chopping frequency of radiation or the thickness of the coupling fluid. It has been shown that, the thickness scanning procedure leads to more accurate results and it is preferred. Consequently, if we apply the TWRC method [8, 9] (this means that we perform a scan of the phase or amplitude of the signal as a function of coupling fluid's thickness, at constant chopping frequency), we can obtain the thermal effusivity of the backing liquid.

When working in the back configuration, in the thermally thick regime of the pyroelectric or TE sensor and sample, we obtain in both cases the same result [4, 7, 10].

$$V^{BPPE} = V_n^{BPTE} = \frac{2}{(b_{12}+1)}\exp(-\sigma_1 l_1) \qquad (10)$$

The normalization in the case of PTE experiment being performed with the empty sensor.

Eq. (10) indicates that a similar scan of the phase or amplitude of the BPPE/BPTE signal as a function of the thickness of the liquid layer 1 (at constant chopping frequency) can lead to the direct measurement of sample's thermal diffusivity.

3. EXPERIMENT

The experimental setups for PPE/PTE experiments in both front and back configurations are extensively described elsewhere [7, 12-13]. The pyroelectric sensor is a $LiTaO_3$ single crystal (15 mm diameter and 215 μm (FPPE) -500 μm (BPPE) thicknesses). The PTE sensor consists of high density sintered pellets (15 mm diameter and 460 μm thickness) of TiS_3 with a Seebeck coefficient of about - 600 μV/K. Both sensors are provided with gold electrodes on both faces.

In the front configuration, the sensor is glued onto a rotating stage. The backing material is situated on a micrometric stage. The modulated radiation (800 mW YAG laser, f = 1Hz) is partially absorbed by the (blackened) front electrode of the sensor. The space between the sensor and the backing material accommodates the coupling fluid. The coupling fluid's thickness variation is performed with a step of 0.03μm (9062M-XYZ-PPP Gothic-Arch-Bearing Picomotor) and the data acquisition is recorded at the end of each 30-th step. The "rough" control of the thickness and the parallelism between backing and sensor are assured by 3 and 6 –axis micrometric stages. During the scanning procedure, the sample's thickness variation was very rigorously controlled, but the absolute sample's thickness was not precisely known. Its correct value was obtained as a result of a fitting procedure [13]. The coupling fluid was water (e_2= 1600Ws$^{1/2}$m^{-2}K^{-1}; α_2= 14.24x10^{-8}m^{2}s^{-1}) with thickness ranging from 0 to 1mm. The normalized signal was obtained with thermally thick (thickness larger than 700μm) coupling fluid. For the above mentioned values of chopping frequency, the requirement imposed by this investigation (thermally thin regime for the sensor and thermally thick for the backing) was respected. The coupling fluid changes the thermal regime from thermally thick to thin at about 400 μm – 600 μm, depending on the chopping frequency. The information was collected in the thermally thin regime for the coupling fluid. All the measurements were performed at room temperature. The PPE/PTE signals were processed with a SR 830 lock-in amplifier. The signal to noise ratio was better than 100.

The liquids under investigation accommodate a special designed cell, preventing leakage and vaporization [14]. The separator between the coupling fluid and the magnetic nanofluid was a 110 μm thick glass window. The liquid samples were magnetic nanofluids with transformer oil as carrier liquid, oleic acid as surfactant and Fe_3O_4 nanoparticles. They have been investigated as a function of nanoparticles' concentration, which was increased from 0.156 mg Fe_3O_4/ ml fluid to 0.623 mg Fe_3O_4/ ml fluid.

In the back detection configuration, the thermal diffusivity of magnetic nanofluids was measured using the same TWRC scanning procedure. The incident light was absorbed in this case by a thin blackened metallic layered in contact with the liquid. The chopping frequency of radiation was 1Hz for PTE and 2Hz for PPE.

4. RESULTS

The results obtained for the phase of the FPPE/FPTE-TWRC signal, for the magnetic nanofluids

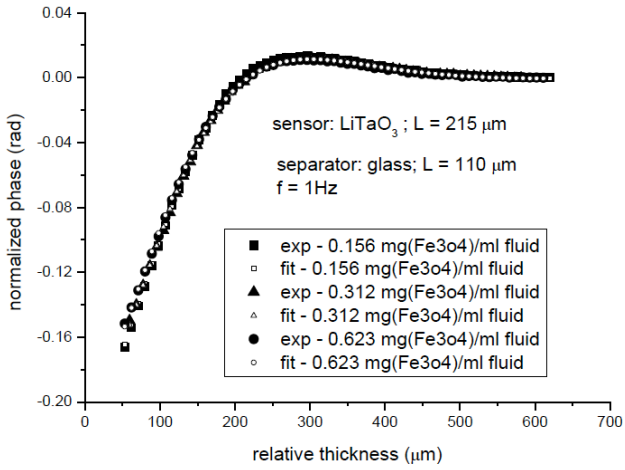

Figure 2: Normalized phase of the FPPE signal as a function of coupling fluid's (water) thickness, for magnetic nanofluids with various Fe_3O_4 concentrations. The best fit is also displayed (small empty circles).

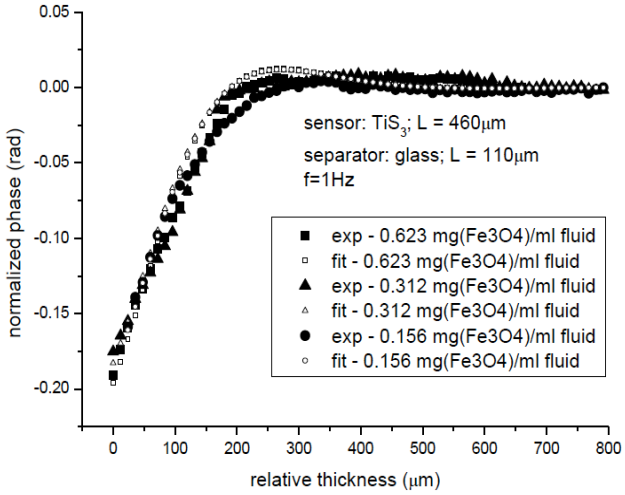

Figure 3: Normalized phase of the FPTE signal as a function of coupling fluid's (water) thickness, for magnetic nanofluids with various Fe_3O_4 concentrations. The best fit is also displayed (small empty circles).

with different magnetic nanoparticles' concentration are displayed in Figures **2** and **3**; the results obtained for the room value of thermal effusivity in Table **1**.

There are no errors inserted in Table **1**, because, for this type of investigations, the accuracy of the results depends on many parameters and it is usually described by a precision map. However, having in mind that the values of the thermal effusivity for the investigated sample (nanofluid) and coupling fluid (water) are rather close, the accuracy of the results is good [13, 14].

The behavior of the phase of the BPPE/BPTE signal (in the thermally thick regime for both sample and sensor), as a function of the sample's thickness, for the magnetic nanofluids, are presented in Figures **4** and **5**.

The results obtained for the values of thermal diffusivity (fitting procedure using Eq. (8)) are presented in Table **2**.

CONCLUDING REMARKS

Two contact photothermal methods, the classical PPE calorimetry and the recently introduced PTE method are proposed, and used for the first time together, for thermal characterization of liquids. In both techniques the back and front detection configurations, together with the TWRC scanning procedure, have been used in order to measure the thermal diffusivity and effusivity of a particular magnetic nanofluid: carrier liquid - transformer oil, surfactant - oleic acid, nanoparticles' type - Fe_3O_4.

Concerning the nanofluid under investigation, there are some literature data, obtained by using the PPE calorimetry which refer to the dependence of the thermal parameters as a function of type of carrier liquid, type of surfactant and type of magnetic nanoparticles [15]. This is why, in this paper, the measurements were performed as a function of nanoparticles' concentration. Both dynamic thermal parameters, the thermal diffusivity and effusivity were obtained by using as source of information the phase of the PPE and PTE signals. Small increases of thermal diffusivity and effusivity with increasing nanoparticles' concentration are observed.

Table 1: The Values of the Thermal Effusivity for the Investigated Magnetic Nanofluids, as Obtained by PTE and PPE Methods, in Front Detection Configuration

sample	Therm. eff. ($Ws^{1/2}\ m^{-2}K^{-1}$)	Therm. eff. ($Ws^{1/2}\ m^{-2}K^{-1}$)
	PTE phase	PPE phase
0.156 mg(Fe_3O_4)/ml fluid	450	460
0.312 mg(Fe_3O_4)/ml fluid	480	480
0.623 mg(Fe_3O_4)/ml fluid	520	530

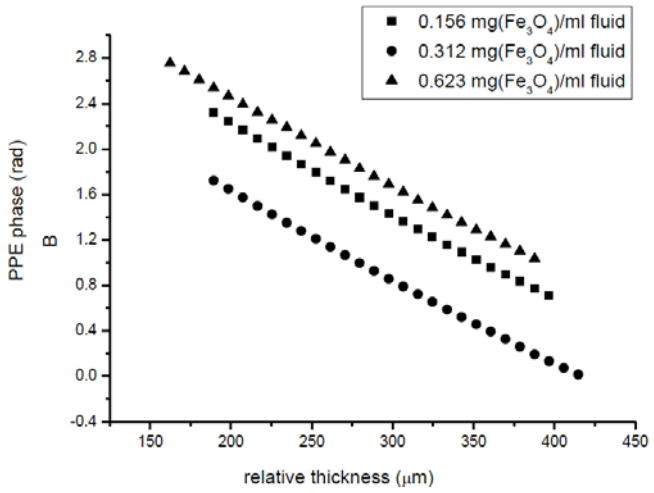

Figure 4: Relative phase of the PPE signal, in back configuration, as a function of nanofluid's thickness, for magnetic nanofluids with various Fe_3O_4 concentrations. The chopping frequency of incident radiation was 2Hz.

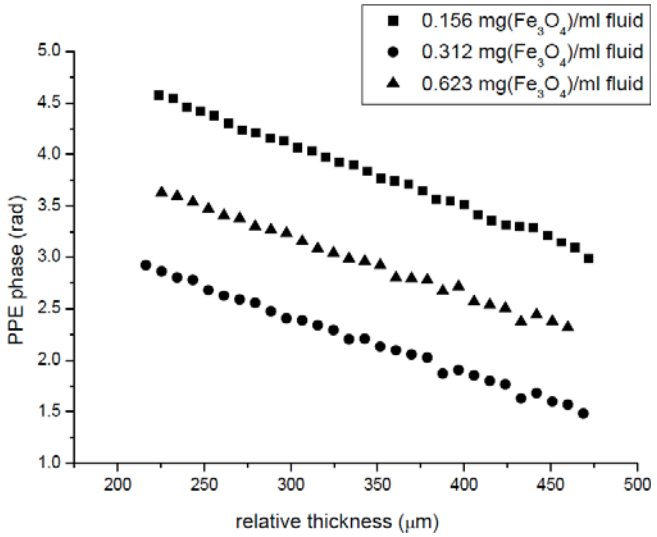

Figure 5: Phase of the PTE signal, in back configuration, as a function of nanofluid's thickness, for magnetic nanofluids with various Fe_3O_4 concentrations. The chopping frequency of incident radiation was 1Hz.

As presented in Figures (**2**) - (**3**) and (**4**) – (**5**) and in Tables **1** and **2**, a comparison of the two methods shows that PTE and PPE give similar results but, for the moment, PPE is more accurate.

Even if the thermoelectrics, as radiation sensors, are an alternative not so performant yet compared with pyroelectrics, this new PTE method has some advantages. First, it is based on cheap, largely available and intensively studied class of sensors. The TE generators are not limited by any critical temperature, as in the case of pyroelectric sensors (Curie point). An additional predicted advantage of PTE technique is the absence of the piezoelectric signal, disturbing sometimes the PPE investigations at high frequencies and/or low temperatures.

As main limitations, concerning this particular thermoelectric material (TiS_3) we mention its chemical reactivity with the deposited electrical contacts (in time) and with atmosphere and moisture at temperatures higher than about 100^0C.

The large effort made during last years in improving the performances of TE generators supports the idea that, in the next future, TE sensors can become competitive with pyroelectric sensors. The main direction in improving the performances of the TE generators *as radiation sensors* is the increase of the Seebeck coefficient.

At the end I want to mention that both contact techniques, described in this paper, are able to directly measure two dynamic thermal parameters, the thermal diffusivity and effusivity. On the other hand, it is well known that the four thermal parameters are connected by two relationships; the direct measurement of two of them leads automatically to the possibility of calculating the remaining two (thermal conductivity and volume specific heat).

In the same time I want to point out that the growing interest in contact PT calorimetric investigations of

Table 2: The Values of the Thermal Diffusivity for the Investigated Magnetic Nanofluids, as Obtained by PTE and PPE Methods, in Back Detection Configuration. The Value of Thermal Diffusivity of Water was also Inserted in Table 2

sample	Thermal diffusivity x10^8 (m^2s^{-1})	Thermal diffusivity x10^8 (m^2s^{-1})
	PTE phase	PPE phase
water	14.29±0.43	14.24±0.25
0.156 mg(Fe_3O_4)/ml fluid	9.33±0.32	9.48±0.19
0.312 mg(Fe_3O_4)/ml fluid	9.70±0.67	10.22±0.26
0.623 mg(Fe_3O_4)/ml fluid	9.84±0.49	10.33±0.51

liquids is due not only to the high sensitivity, stability and reproducibility of the methods, but also to the simplicity of the detection cells and laboratory instrumentation involved.

ACKNOWLEDGEMENT

Work supported in part by the Romanian Ministry of Education and Research Youth and Sport, through the National Research Programs, PN-II-ID-PCE-2011-3-0036 and PN-II-PT-PCCA-2-11-3. The author wants to thank Prof. E. Guilmeau and Drs. L. Vekas and R. Turcu for delivering TE materials and nanofluid samples.

REFERENCES

[1] Mandelis A. Principles and perspectives of photothermal and photoacoustic phenomena. Elsevier NY. 1992.

[2] Mandelis A, Zver MM. Theory of the photopyroelectric effect in solids. J Appl Phys 1985; 57: 4421-4430. http://dx.doi.org/10.1063/1.334565

[3] Chirtoc M, Mihailescu G.Theory of the photopyroelectric method for investigation of optical and thermal materials properties. Phys Rev 1989; B 40: 9606-9617.

[4] Dadarlat D, Neamtu C. High performance photopyroelectric calorimetry of liquids. Acta Chim Slov 2009; 56: 225-236.

[5] Dadarlat D, Streza M, Pop MN, Tosa V, Delenclos S, Longuemart S, and Sahraoui AH. Photopyroelectric calorimetry of solids. FPPE-TWRC method. J Therm Anal Calorim 2010; 101: 397-402. http://dx.doi.org/10.1007/s10973-009-0513-6

[6] Kuriakose M, Depriester M, King RCY, Rousel F, Sahraoui AH. Photothermoelectric effect as a novel approach to investigate thermal parameters of carbon nanotube/polyaniline based materials. J Appl Phys 2013; 113: 044502. http://dx.doi.org/10.1063/1.4788674

[7] Dadarlat D, Streza M, Chan YKR, Roussel F, Kuriakose M, Depriester M, Guilmeau E, Sahraoui AH. The photothermoelectric technique (PTE), an alternative photothermal calorimetry. Meas Sci Technol 2014; 25: 015603. http://dx.doi.org/10.1088/0957-0233/25/1/015603

[8] Shen J, Mandelis A. Thermal-wave resonator cavity. Rev Sci Instrum 1995; 66: 4999-5005. http://dx.doi.org/10.1063/1.1146123

[9] Balderas-Lopez LA, Mandelis A, Garcia JA. Thermal-wave resonator cavity design and measurements of the thermal diffusivity of liquids. Rev Sci Instrum 2001; 71: 2933-2937. http://dx.doi.org/10.1063/1.1150713

[10] Marinelli M, Mercuri F, Zammit U, Pizzoferrato R, Scudieri F, Dadarlat D. Photopyroelectric study of specific heat, thermal conductivity and thermal diffusivity of Cr2O3 at the Neel transition. Phys. Rev. 1994; B49: 9523-9532. http://dx.doi.org/10.1103/PhysRevB.49.9523

[11] Dadarlat D. Contact and non-contact photothermal calorimetry for investigation of condensed matter. Trends and recent developments. J Therm Anal Calorim 2012; 110**:** 27-35. and references therein. http://dx.doi.org/10.1007/s10973-011-2180-7

[12] Streza M, Pop M N, Kovacs K, Simon V, Longuemart S, Dadarlat D. Thermal effusivity investigations of solid materials by using the thermal-wave-resonator-cavity (TWRC) configuration. Theory and mathematical simulations. Laser Phys 2000; 19: 1340-1344. http://dx.doi.org/10.1134/S1054660X09060267

[13] Dadarlat D. Photopyroelectric calorimetry of liquids. Laser Phys 2009; 19: 1330-1340. http://dx.doi.org/10.1134/S1054660X09060255

[14] Dadarlat D, Pop MN. Self-consistent Photopyroelectric Calorimetry for Liquids. Int J Thermal Sciences 2012; 56: 19-22. http://dx.doi.org/10.1016/j.ijthermalsci.2012.01.015

[15] Dadarlat D, Neamtu C**,** Streza M, Turcu R, Craciunescu I, Bica D, Vekas L. High Accuracy Photopyroelectric Investigation of Dynamic Thermal Parameters of Fe3O4 and CoFe2O4 Nanofluids. J Nanoparticles Res 2008; 10: 1329-35. http://dx.doi.org/10.1007/s11051-008-9386-z

Received on 04-09-2014 Accepted on 23-09-2014 Published on 17-10-2014

DOI: http://dx.doi.org/10.15377/2409-5826.2014.01.01.2